Journal of Materials Chemistry A

Accepted Manuscript

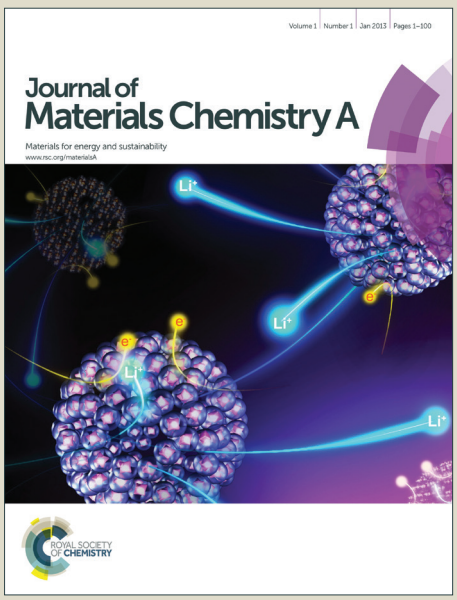

ROYAL SOCIETY OF CHEMISTRY

www.rsc.org/materialsA

Hollow Nanospheres of Loosely Packed Si/SiOx Nanoparticles Encapsulated in Carbon Shells with Enhanced Performance as Lithium Ion Battery Anodes

Wenyue Li, Zhangpeng Li, Wenpei Kang, Yongbing Tang, Zhenyu Zhang, Xia Yang, Hongtao Xue, and Chun-Sing Lee**

Dr. Yongbing Tang, Dr Wenyue Li
Functional Thin Films Research Center
Shenzhen Institutes of Advanced Technology, Chinese Academy of Sciences
Shenzhen, 518055, China
Email: tangyb@siat.ac.cn

Professor Chun-Sing Lee, Dr. Wenyue Li, Dr. Zhangpeng Li, Dr. Yongbing Tang, Dr. Wenpei Kang, Dr. Xia Yang, Zhenyu Zhang, Hongtao Xue
Department of Physics and Materials Science
Center of Super-Diamond and Advanced Films (COSDAF)
The City University of Hong Kong
Hong Kong SAR (China)
Email: apcslee@cityu.edu.hk

Abstract: Silicon materials are considered as the new generation of high specific energy and energy density anode for rechargeable lithium ion batteries, but the silicon pulverization during lithium insertion hinders its commercial implementation. Although extensive effort has been put on addressing these problems, the microstructure of silicon material still needs to be well engineered in order to improve the stability of the anode materials and simplify the synthesize procedure using scalable and easy available silicon source without any toxicity. In this work, a novel hollow nanosphere with Si/SiOx nanoparticles incompactly distributed within a spherical carbon shell was successfully fabricated via a facile *in-situ* carbonization/reduction method. With enhanced electrode conductivity and sufficient free space for silicon expansion during the lithiation process, this material shows

much better cycle lives and rate capability than directly reduced silicon nanoparticles.

1. Introduction

Lithium ion batteries (LIBs) have been considered as one of the most promising energy storage devices due to their intrinsic advantages of high energy density, high efficiency, superior rate capability and long cycling life.[1-4] But the existing LIB technology based on graphite anode is reaching its performance limit due to its relatively low theoretical capacity of 370 mAh g^{-1}. [5-9] To address this issue, various anode materials with higher specific energy including transition metal oxide/sulfide,[10-15] intermetallic compounds,[16] silicon-based[17-19] and tin-based [20, 21] materials have been explored. Among these anode materials, silicon has remarkably high theoretical capacity of about 4200 mAh g^{-1} and has attracted many attentions.[22] However, performance and stability of silicon-based anodes are limited by their intrinsically low electronic conductivity and large volume changes during lithium insertion/extraction.[23] In particular, the large volume change can cause the pulverization of the silicon anode, which leads to loss of electrical contact with current collector and rapid capacity fading.[22] Extensive research has been put on addressing these challenges, typically by engineering well-designed silicon nanostructures including nanoparticles,[24-28] nanowires,[29,30] nanotubes,[31,32] nanospheres,[33,34] films[35,36] as well as incorporating carbon/graphene as conducting pathway and mechanical cushion.[37,38]

Based on these pioneering works, ideal microstructure of silicon-based anode should have several important attributes. Firstly, there should be empty space around silicon

nanostructure for accommodation the volume change for reducing the chance of pulverization.[24,27,38,39] The most successful way for engineering empty space is typically a three-step approach: 1) growth of SiO_2 on Si; 2) coating of the Si/SiO_2 core/shell structure with carbon materials or polymers; 3) creation of empty space by chemical etching way the SiO_2 layer. Another important requirement is that the anode should contain enough amount of highly conducting material for forming a conducting network. Due to the intrinsically low conductivity of silicon, this requirement suggests that a composite system should be used. So far carbon-based materials such as graphene, carbon nanotube or conducting polymer are commonly used.[37,38,40] Another requirement concerns the contact area between the electrolyte and the silicon-based anode. However, there is a dilemma that while a large contact area between the anode and the electrolyte is beneficial for high rating performance; a large silicon/electrolyte contact area would lead to a large amount of solid electrolyte interface (SEI) which is harmful for the columbic efficiency and cycling stability. The solution to this dilemma is to void direct contact between silicon and the electrolyte while providing access of lithium ion to the silicon material. These requirements are basically satisfied by a Si:C composite recently reported by Cui et al [22,40]. They successful obtained a core-shell structure in which commercial silicon nanoparticles are encapsulated in a carbon shell with enough free spaces via the mentioned three-step approach. Other than this method, there are so far little reports on Si-based anode satisfying the above requirements.

Here, we report a novel microstructure and synthesis approach of Si:C composite for

LIB applications. The composite exhibits a hollow structure in which many loosely-packed Si/SiOx nanoparticles are encapsulated in a single carbon shell, according with the requirements for Si as LIB anode. Especially, this nanostructure can be easily produced in large scale with a controllable approach at low cost without using cost intensive process (e.g. chemical vapor deposition) or toxic reagent (e.g. $SiCl_4$ or SiH_4 etc).

2. Experimental

Synthesis of SiO_2 nanospheres

The traditional Stöber method via hydrolyzing reaction of tetraethyl orthosilicate (TEOS) was used here to prepare the SiO_2 nanospheres [41]. In a typical process, 6 mL of TEOS was added into a mixture of 140 mL ethanol, 20 mL deionized water and 3 mL ammonia. The mixture was hydrolyzed and condensed for 3 hours under moderate stirring. The sample was then centrifuged and washed sequentially with deionized water and ethanol. SiO_2 nanospheres were finally obtained after drying at 100 ^{o}C and calcination at 550 ^{o}C for 6 h in the air atmosphere in order to get rid of the organic residues and make their structures more stable during the following directly reduction treatment.

Preparation of the hollow nanospheres

The synthesis process of the hollow nanospheres is schematically shown in Figure 1. First, 0.3 g of the SiO_2 was uniformly dispersed in dimethylformamide (DMF) under sonication. 0.1 g of polyacrylonitrle (PAN) was then added into dispersion with a few drops of 3-aminopropyltriethoxysilane (APTES) as a coupling agent. The DMF

solvent was then evaporated by heating the sample to 140 ^{o}C under intensively stirring. To pre-oxidize the polymer for forming the carbon precursor, the sample was placed in a muffle furnace and treated at 250 ^{o}C for 2 h. The sample was then homogeneously mixed with magnesium powder and loaded into a corundum boat. The sample was heated in a tube furnace at 800 ^{o}C for 3 h with a steady flow of 5% H_2 in Ar. After cooling, the sample was stirred in a 2 M HCl solution for 2 h at room temperature to remove the magnesia. Finally, the sample was filtrated and washed with deionized water until pH~7. The hollow nanosphere was finally obtained by drying under vacuum at 60 ^{o}C for 8 h. For comparison, unencapsulated Si nanopartilce were similarly prepared except skipping the PAN coating process.

Characterization

Scanning electron microscopy (SEM) images were carried out on a Philips XL30 FEG SEM. Transmission electron microscopy (TEM), selected area electron diffraction (SAED), electron energy loss spectroscopy (EELS) and high-resolution TEM (HRTEM) were carried out on a JEM-2100F electron microscope operating at 200 kV. X-ray diffraction (XRD, Philips X'Pert) patterns of the samples were acquired using CuK_{α} radiation. Raman spectroscopy was carried out with a Renishaw 2000 Raman microscope with a laser wavelength of 633 nm.

Electrochemical characterization

Anodes of LIBs were prepared through the following steps: active materials (the hollow nanospheres or the unencapsulated Si nanoparticles), conductivity agent (carbon black) and binder (sodium carboxymethylcellulose, CMC) in a weight ratio of

70:20:10 were blended with deionized water. Anodes were prepared by coating the mixture on a copper foil and vacuum-dried at 60 ^{o}C for 12 h. Coin-type cells were fabricated using lithium metal as the counter electrode, Celgard 2400 as the separator, and $LiPF_6$ (1 M) in ethylene carbonate/dimethyl carbonate (EC/DMC, 1:1 vol %) as the electrolyte. Assembled cells were aged for 24 h in an Ar-filled glove (MBRAUN) before test. Cyclic voltammetry (CV) measurement was conducted at 0.1 mV s^{-1} over the range of 0.01-1.0 V (vs Li/Li^+) on a CHI 600D electrochemical workstation. Electrochemical impedance spectroscopy (EIS) was carried out with the ZAHNER-elektrik IM 6 electrochemical system over a frequency range of 100 kHz to 10 mHz. Cycling of cells was tested over a fixed voltage window of 0.01-1.0 V (vs Li/Li^+) with a battery test system (MACCOR 4000) at room temperature. To study the microstructural change upon cycling, a battery with the hollow nanosphere anode was dissembled after 50 cycles, and anode was washed sequentially with deionized water, ethanol and acetone. After drying in vacuum, the samples were collected for TEM observation.

3. Results and discussion

Overall strategy for preparation of the hollow nanosphere is schematically depicted in Figure 1. SiO_2 nanospheres of about 180 nm diameter were firstly prepared by hydrolyzing reaction of tetraethyl orthosilicate (TEOS), [41] and then ultrasonically dispersed in dimethylformamide (DMF). Polyacrylonitrle (PAN) was dissolved into the dispersion together with 3-aminopropyltriethoxysilane (APTES) as a coupling agent. APTES molecular can be easily grafted onto the SiO_2 nanosphere surface due

to its oxygen-containing functional groups (e.g. Si-O-Si bond). Upon evaporation of solvent under vigorous stirring, the PAN molecules would assemble onto the nanospheres through interaction between their nitrile groups and the amine groups of APTES. The PAN coated nanospheres were then pre-oxidized in air to further stabilize the polymer coating.[42] The polymer coated SiO_2 spheres were then homogenously mixed with magnesium powder and annealed at 800 ^oC in a reducing atmosphere. During this one step annealing, there are simultaneously structural, chemical and morphological changes on the polymer coated SiO_2 sphere leading directly to the final product of the hollow nanospheres. While the polymer shell is carbonized, SiO_2 is reduced to Si. Due to the substantial volume reduction, each SiO_2 nanosphere disintegrated into many loosely packed Si nanoparticles of a few nanometers size which closely attach on the inwall of carbon shell, leading to the hollow nanosphere strucutre. Comparing to the previously reported Si nanostructures,[37, 39, 43] the uniqueness of the present process is that the whole assembly of carbon shell, Si nanoparticles and the surrounding space are achieved by one step.

Morphology and microstructure of the as-prepared samples were characterized by scanning electron microscope (SEM) and transmission electron microscope (TEM). A typical SEM image (Figure 2a and S1a) shows that the as-prepared SiO_2 nanospheres have a uniform spherical morphology with an average diameter of ~180 nm. After polymer coating and subsequent carbonization, the average diameter was slightly increased to ~200 nm (Figure 2b). Hollow feature can be observed from most of the

spheres (marked with arrows in Figure 2b). TEM investigation further confirms the structure of the as-synthesized nanospheres (Figure 2c). It can be seen that the spherical cages contain many loosely packed nanoparticles and have an amorphous shell with a thickness of about 10 nm (Figure 2d, 2e and S2). Upon losing its oxygen atoms upon annealing with magnesium, the SiO_2 nanospheres show substantial volume reduction and each breaks down into many loosely packed nanoparticles within a spherical carbon shell. Most of the reduced nanoparticles in the shells are Si crystal as shown in a typical high-resolution TEM (HRTEM) image (Figure 2f) with lattice spacing match well to the Si {111} spacing.

Electron energy loss spectroscopy (EELS) mappings were carried out to further confirm the element distribution in the nanospheres. EELS mapping analysis (Figure 3a-3d) shows that the outer shell is composed of carbon originated from the PAN coating, while the inner part is mainly composed of disconnected Si, as well as oxygen, indicating existence of SiO_x phase due to incomplete reduction of SiO_2. X-ray diffraction (XRD) patterns in figure 3e confirm that prepared samples with and without the carbon shell consist mainly of crystalline Si and small amount of SiO_2 ($2\theta \approx 22^o$). Si content in the nanospheres is estimated to be about 58 wt.% according to the TGA measurement (Figure S3). Raman spectrum of the hollow nanospheres exhibits a disorder-induced D band at about 1346 cm^{-1}, a graphitic G band at about1595 cm^{-1} (see magnified portion shown in the insert), which are attributed to the outer carbon shell.[44]

Electrochemical performances of the synthesized samples were first evaluated with battery test. Figure 4 shows voltage profiles of the battery with the nanospheres anode at 0.1 A g^{-1} for the first cycle for electrode activation (Figure 4a) and at 1.0 A g^{-1} in the subsequent cycles (Figure 4b). The electrode delivers a capacity of 2350 and 1450 mAh g^{-1} for the first discharge and charge with a Coulombic efficiency of ~65%, which is much better than those of reduced Si sample without the carbon shell (~55%, Figure S4). Irreversible capacity loss mainly caused by the formation of solid electrolyte interface (SEI) layer on the electrode surface and the consumption of lithium ions in the first lithiation process, which are common to most anode materials. [45] Figure 3c compares the cycle capacity and stability of batteries with the nanospheres and the unencapsulated Si nanoparticles. While the unencapsulated Si nanoparticle anode gives a higher initial capacity of 2932 mAh g^{-1}, the capacity drops rapidly to 200 mAh g^{-1} after 100th cycle and its capacity retention with respect to the second cycle is only 21.7%. In contrast, the hollow nanosphere anode demonstrates much better electrochemical reversibility and maintains a capacity of 940 mAh g^{-1} (92% of its capacity w.r.t. 2nd cycle) after 100 cycles. If the SiOx was etched by the HF solution, the cycle stability also becomes very poor (Figure S5, only 465 mAh g^{-1} retention after 100 cycles). It is obvious that this novel structure can effectively improve the cycling stability of the silicon anode.

Furthermore, anode with this hollow nanosphere also exhibits a good rate capability. Figure 4d shows the capacity of the corresponding battery at different current densities (0.2-5.0 A g^{-1}). Even at high rating of 5 A g^{-1}, the capacity is about 630 mAh

g^{-1}, still larger than those of Si nanoparticles and graphite tested at considerably lower current densities.[46,47] Particularly, a capacity of 1050 mA g^{-1} can be resumed as the current density decreased from 5 A g^{-1} to 1 A g^{-1}.

The improved electrochemical performance of hollow nanosphere should be ascribed to its unique microstructure which effectively accommodates the volume expansion, increases contact area with the electrolyte and provides a conducting network. According to previous studies,[22, 39] it is difficult to form stable SEI films for silicon-based anodes because of the repeated volume expansion and contraction, which causes continuously shifting of the interface between silicon and the electrolyte. Figure S6 shows the first five cyclic voltammetry (CV) curves of the electrode made from these nanospheres. The reduction peak at ~ 0.5 V in the first cycle is attributed to the formation of SEI layer on the electrode surface,[48, 49] which is no long appears in the following cycles, indicating a stable SEI layer can be formed in the first cycle. As characterized by the TEM images (Figure 2c, e), the hollow nanostructures composed of spherical carbon cages containing many incompact Si nanoparticles. The voids around each Si nanoparticle provide sufficient space for large volume expansion without structural damage during Li^+ insertion, as illustrated in Figure 5a. Meanwhile, the carbon shells can effectively sustain the whole structure even if the inner Si nanoparticles go through large deformation. This was confirmed by detecting the electrode microstructure after cycling. As shown in Figure 5 and S7, it can be seen that most of the nanospheres still keep a sphere structure after 50 cycles.

We also carried out electrochemical impedance spectroscopy (EIS) measurements to investigate charge transfer mechanisms of this hollow nanostructure in LIBs. The Nyquist plots of the cells with the nanospheres and the directly reduced Si nanoparticles are shown in Figure S8. The diameter of the semi-circle at the high frequency was dramatically decreased in the nanosphere, compared to the directly reduced Si, which is strongly attributed to the increased electrical conductivity of the overall electrode. The charge transfer resistance (R_{ct}) for the nanosphere and the reduced Si were determined to be ~70 and ~300 Ω, respectively. The much lower R_{ct} value of the hollow nanospheres compared to that of Si nanoparticle demonstrates that this Si:C geometric assembly can effectively decrease the charge transfer resistance of Si.

It should be noted that while the performance of the synthesized hollow nanospheres is better or comparable to those Si:C composite anode prepared from SiO_2 (Table S1),[32, 50-53] it is still lower than those of the state-of-the-art Si:C anode prepared from commercial crystalline Si source. [9,17,25] This difference may be related to the incompletely reduction of SiO_2 and the much higher defect densities and oxygen contents in the Si obtained by the reduction process. However, considering the much lower cost of the SiO_2 source comparing to the crystalline Si source (about 30 times in cost per gram) and the facile preparation process, the present approach should have good potential for practical LIB applictions.

4. Conclusions

In summary, we successfully synthesized a hollow nanospheres with incompact Si

nanoparticles encapsulated by carbon shells by an *in-situ* carbonization/reduction process using inexpensive and easily obtainable C and Si sources. As LIB anode, the fabricated hollow nanostructures show much better electrochemical performances than the directly reduced Si nanoparticles, this enhanced performance can be attributed to the sufficient spaces between the Si nanoparticles which effectively accommodate the large volume expansion during lithium ions insertion/extraction. Furthermore, the outer layer carbon shell can increase the conductivity of the whole electrode, and thus significantly decrease the charge transfer resistance of Si anode. We believe that the controllable fabrication process and easily obtainable raw materials for C and Si sources will make this nanostructure promising for scalable practical application of Si for high performance LIBs.

Acknowledgements

This project has been financially supported by National Natural Science Foundation of China (Nos. 51272217, 51302238), Collaboration Project of City University of Hong Kong and ShenZhen Huawei (YB2012090343).

References

[1] J. M. Tarascon, M. Armand, *Nature,* **2001**, *414*, 359.

[2] H. Wang, L. Cui, Y. Yang, H. S. Casalongue, J. T. Robinson, Y. Liang, Y. Cui, H. J. Dai, *J. Am. Chem. Soc.,* **2010**, *132*, 13978.

[3] S. Yang, X. Feng, L. Zhi, Q. Cao, J. Maier, K. Müllen, *Adv. Mater.,* **2010**, *22*, 838.

[4] C. Liu, F. Li, L. Ma, H. M. Cheng, *Adv. Mater.,* **2010**, *22*, E28-62.

[5] P. Poizot, S. Laruelle, S. Grugeon, L. Dupont, J. M. Tarascon, *Nature,* **2000**, *407*,

496.

[6] G. Zhou; D. Wang, F. Li, L. Zhang, N. Li, Z. Wu, L. Wen, M. Lu, H. M. Cheng, *Chem. Mater.,* **2010**, *22*, 5306.

[7] P. R. Abel, Y. M. Lin, H. Celio, A. Heller, C. B. Mullins, *ACS Nano,* **2012**, *6*, 2506.

[8] X. Zhou, L. Wan, Y. G. Guo, *Adv. Mater.,* **2013**, *25*, 2152.

[9] H. Wu, Y. Cui, *Nanotoday,* **2012**, *7*, 414.

[10] X. W. Lou, Y. Wang; C. Yuan, J. Y. Lee, L. A. Archer, *Adv. Mater.,* **2006**, *18*, 2325.

[11] Y. Du, Z. Yin, X. Rui, Z. Zeng, X. Wu, J. Liu, Y. Zhu, J. Zhu, X. Huang, Q. Yan, H. Zhang, *Nanoscale*, **2013**, 5, 1456.

[12] R. Hu, W. Sun, H. Liu, M. Zeng, M. Zhu, *Nanoscale*, **2013**, 5, 11971.

[13] X. Cao, Y. Shi, W. Shi, X. Rui, Q. Yan, J. Kong, H. Zhang, *Small,* **2013**, *9*, 3433.

[14] W. Zhou, X. Cao, Z. Zeng, W. Shi, Y. Zhu, Q. Yan, H. Liu, J. Wang, H. Zhang, *Energy Environ. Sci.,* **2013**, *6*, 2216.

[15] J. Wang, N.Yang, H. Tang, Z. Dong, Q. Jin, M. Yang, D. Kisailus, H. Zhao, Z. Tang, D. Wang, *Angew. Chem. Int. Ed.,* **2013**, *52*, 6417.

[16] R. Benedek, M. M. Thackeray, *J. Power Sources,* **2002**, *110*, 406.

[17] T. H. Hwang, Y. M. Lee, B. Kong, J. Seo, J. W. Choi, *Nano Lett.,* **2012**, *12*, 802.

[18] X. Li, L. Zhi, *Nanoscale*, **2013**, 5, 8864.

[19] T. Song, J. Xia, J. H. Lee, D. H. Lee, M. S. Kwon, J. M. Choi, J. Wu, S. K. Doo, H. Chang, W. II Park, *Nano Lett.,* **2010**, *10*, 1710.

[20] D. Larcher, S. Beattie, M. Morcrette, K. Edström, J.-M. Jumas, J.-C. Tarascon, *J. Mater. Chem.*, **2007**, *17*, 3759.

[21] J. Chen, D. Luan, C. Li, F. Y. C. Boey, S. Z.Qiao, X. W. Lou, *Chem. Comm.,* **2010**, *46*, 8252.

[22] C. Chan, H. Peng, G. Liu, K. McIlwrath, X. Zhang, R. A. Huggins, Y. Cui, *Nat. Nanotech.,* **2008**, *3*, 31.

[23] C. M. Park, J. H. Kim, H. Kim, H. J. Sohn, *Chem. Soc. Rev.,* **2010**, *39*, 3115.

[24] S. Iwamura, H. Nishihara, T. Kyotani, *J. Phys. Chem. C,* **2012**, *116*, 6004.

[25] B. Liu, P. Soares, C. Checkles, Y. Zhao, G. Yu, *Nano Lett.,* **2013**, *13*, 3414.

[26] D. S. Jung, T. H. Hwang, S. B. Park, J. W. Choi, *Nano Lett.,* **2013**, *13*, 2092.

[27] H. Kim, B. Han, J. Choo, J. Cho, *Angew. Chem. Int. Ed.,* **2008**, *47*, 10151.

[28] B. Koo, H. Kim, Y. Cho, K. T. Lee, N. S. Choi, J. Cho, *Angew. Chem. Int. Ed.,* **2012**, *124*, 8892.

[29] L.-F. Cui, R. Ruffo, C. K. Chan, H. Peng, Y. Cui, *Nano Lett.,* **2009**, *9*, 491.

[30] M. Ge, J. Rong, X. Fang, C. Zhou, *Nano Lett.,* **2012**, *12*, 2318.

[31] B. Hertzberg, A. Alexeev, G. Yushin, *J. Am. Chem. Soc.,* **2010**, *132*, 8548.

[32] J.-K. Yoo, J. Kim, Y. S. Jung, K. Kang, *Adv. Mater.,* **2012**, *24*, 5452.

[33] H. Ma, F. Cheng, J. Chen, J. Zhao, C. Li, Z. Tao, J. Liang, *Adv. Mater.,* **2007**, *19*, 4067.

[34] Y. Yao, M. T. McDowell, I. Ryu, H. Wu, N. Liu, L. Hu, W. D. Nix, Y. Cui, *Nano Lett.,* **2011**, *11*, 2949.

[35] J. Maranchi, A. Hepp, P. Kumta, *Elelctrochem. Solid-State Lett.,* **2003**, *6*, A198.

[36] L.-F. Cui, L. Hu, J. W. Choi, Y. Cui, *ACS Nano,* **2010**, *4*, 3671.

[37] X. Zhou, Y. Yin, L. Wan, Y. G. Guo, *Adv. Energy Mater.,* **2012**, *2*, 1086.

[38] B. Wang, X. Li, X. Zhang, B. Luo, Y. Zhang, L. Zhi, *Adv. Mater.,* **2013**, *25*, 3560.

[39] H. Wu, G. Zheng, N. Liu, T. J. Carney, Y. Yang, Y. Cui, *Nano Lett.,* **2012**, *12*, 904.

[40] N. Liu, Z. Lu, J. Zhao, M. T. McDowell, H.-W. Lee, Y. Cui, *Nat. Nanotech.,* **2014**, 9, 187.

[41] W. Stöber, A. Fink, E. Bohn, *J. Colloid Interface Sci.,* **1968**, *26*, 62.

[42] X. Qin, Y. Lu, H. Xiao, Y. Hao, D. Pan, *Carbon,* **2011**, *49*, 4598.

[43] S. Chen, M. L. Gordin, R. Yi, G. Howlett, H. Sohn, D. Wang, *Phys. Chem. Chem. Phys.,* **2012**, *14*, 12741.

[44] Q. Cheng, M.Wu, M. Li, L. Jiang, Z. Tang, *Angew. Chem. Int. Ed.,* **2013**, *52*, 3750.

[45] S. Yang, X. Feng, L. Zhi, Q. Cao, J. Maier, K. Müllen, *Adv. Mater.,* **2010**, *22*, 838.

[46] H. Xiang, K. Zhang, G. Ji, J. Lee, C. Zou, X. Chen, J. Wu, *Carbon,* **2011**, *49*, 1787.

[47] Y. Yu, L. Gu, C. Zhu, S. Tsukimoto, P. A. V. Aken, J. Maier, *Adv. Mater.,* **2010**, **22**, 2247.

[48] Y. Xu, G. Yin, Y. Ma, P. Zuo, X. Cheng, *J. Mater. Chem.,* **2010**, *20*, 3216.

[49] V. P. Phan, B. Pecquenard, F. L. Cras, *Adv. Funct. Mater.,* **2012**, *22*, 2580.

[50] S. Chen, P. Bao, X. Huang, B. Sun, G. Wang, *Nano Res.,* **2014**, *7*, 85.

[51] X. Liu, Y. Gao, R. Jin, H. Luo, P. Peng, Y. Liu, *Nano Energy,* **2014**, *4*, 31.

[52] A. Xing, J. Zhang, Z. Bao, Y. Mei, A. S. Gordin, K. H. Sandhage, *Chem. Commun.,* **2013**, *49*, 6347.

[53] Y. Ma, G. Ji, B. Ding, J. Y. Lee, J. Mater. Chem. A, **2013**, *1,* 13625.

Figures

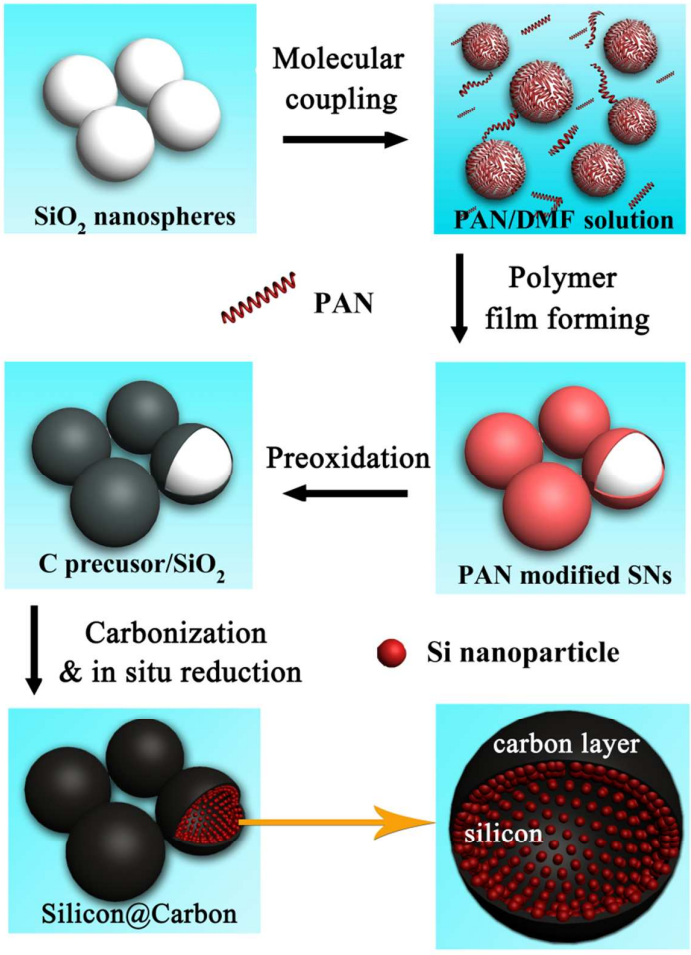

Figure 1. Schematic illustration of the fabrication process of silicon@carbon hollow nanospheres.

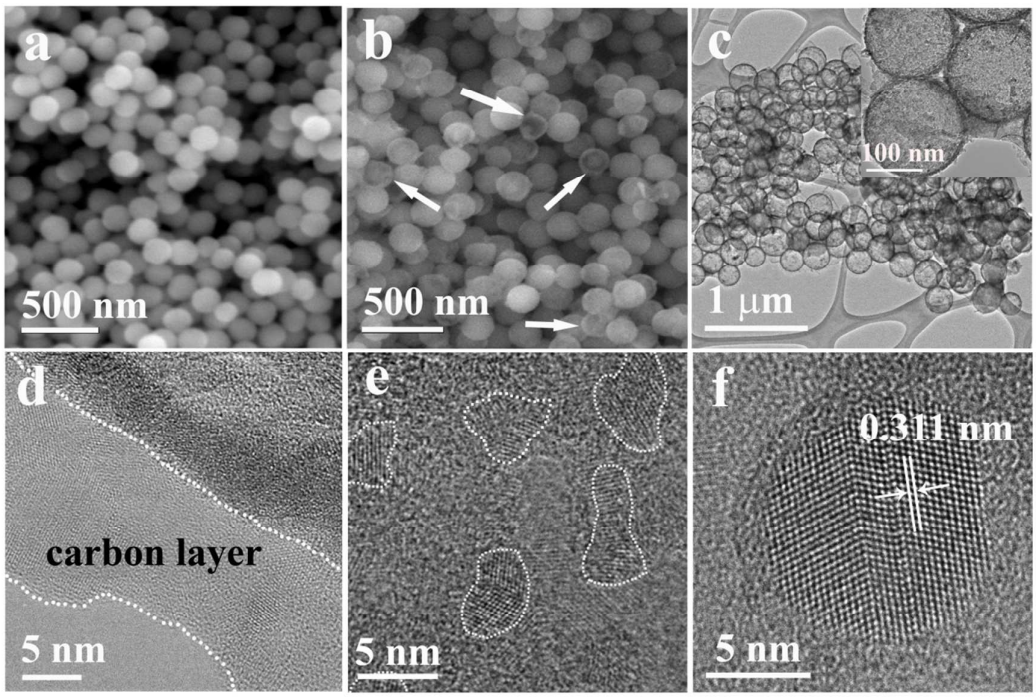

Figure 2. Figure 2 SEM images of the as-prepared SiO_2 nanospheres (a) and hollow nanospheres (b). TEM (c) and HRTEM (d, e, f) images of the hollow nanospheres.

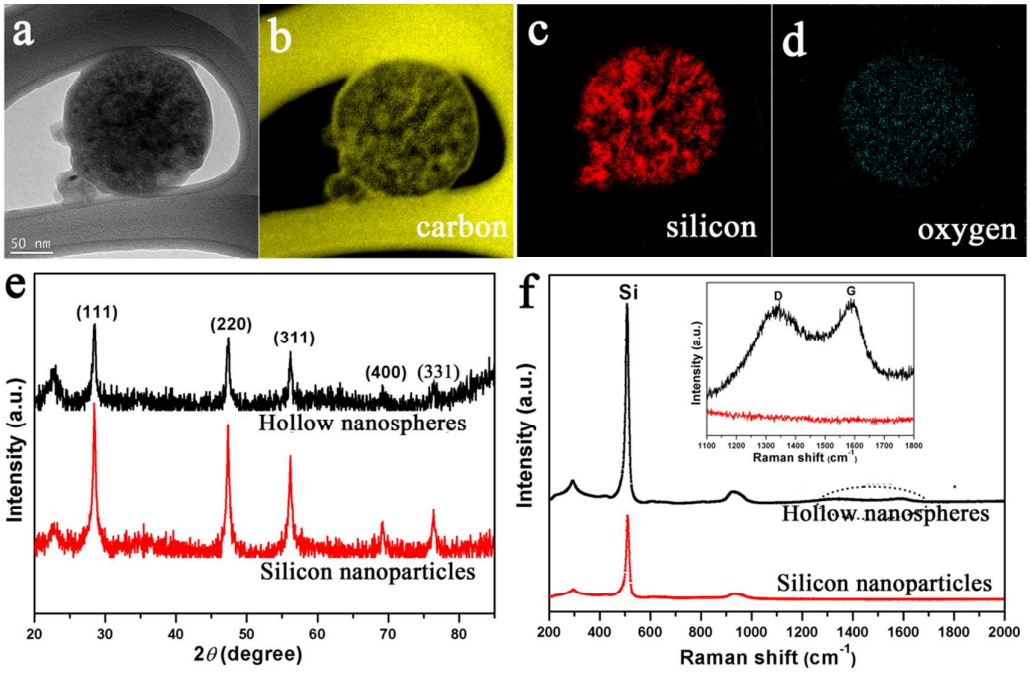

Figure 3. Electron energy loss spectroscopy (EELS) elemental mapping images of a typical hollow nanosphere for carbon (b), silicon (c) and oxygen (d) elements. XRD patterns (e) and Raman spectra (f) of directly reduced Si nanopartilce and hollow nanospheres.

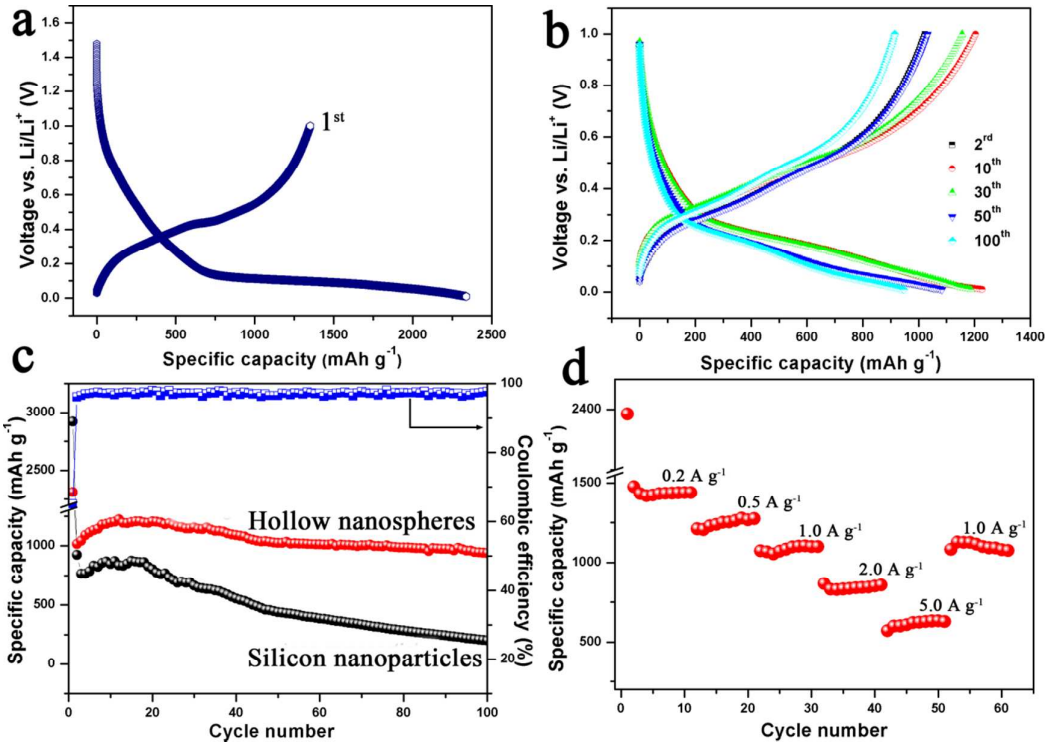

Figure 4. Voltage profiles plotted for the 1st cycle at the current density of 0.1 A g^{-1} (a) and 2nd, 10th, 30th, 50th and 100th cycles at a current density of 1.0 A g^{-1} (b). Charge-discharge capacities of the hollow nanospheres and directly reduced Si nanoparticles at a current density of 1 A g^{-1} (c). hollow nanospheres electrode at different rates ranging from 0.2 A g^{-1} to 5 A g^{-1}(d).

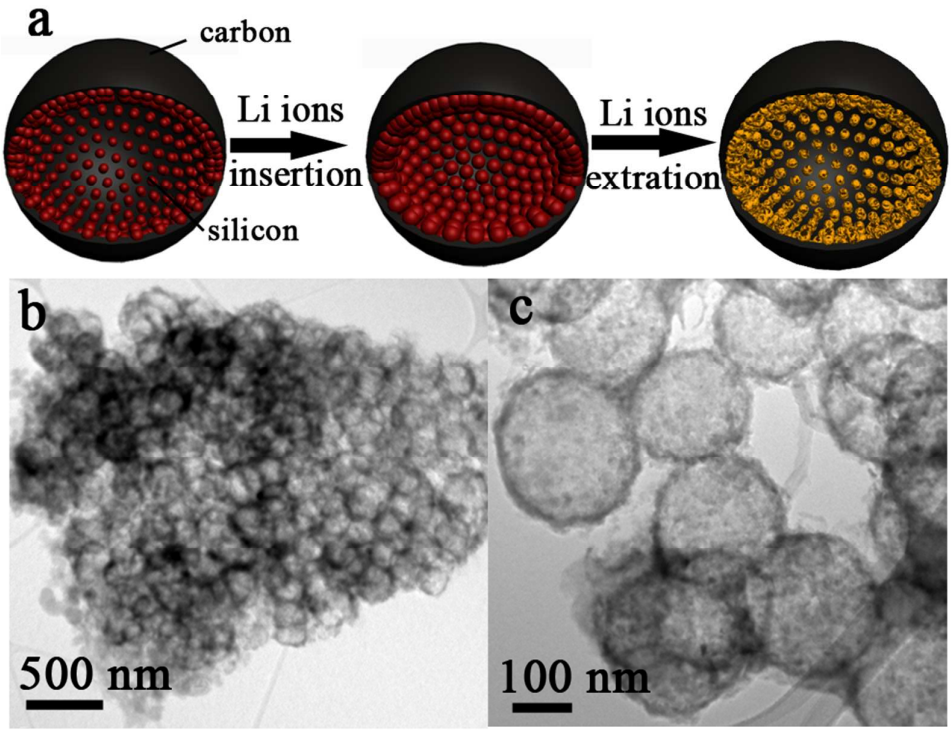

Figure 5. Schematic illustration of the deformation of hollow nanospheres during the lithiation and delithiation processes (a).TEM (b and c) images of hollow nanospheres after 50 cycles.

ToC figure

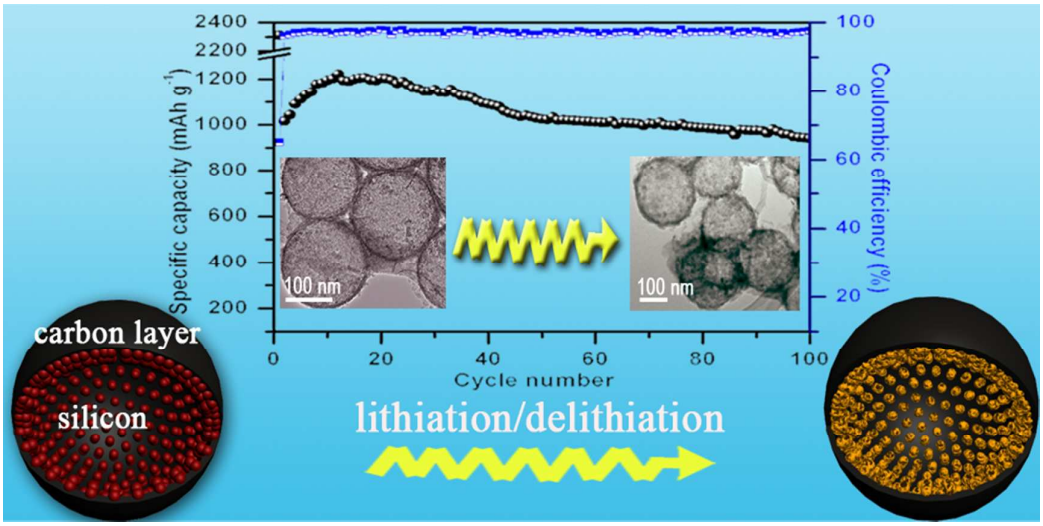

A novel hollow Si/C nanospheres with enhanced lithium ion battery performance was successfully fabricated via a facile in-situ carbonization/reduction method.